Atlantic Journal of Life Sciences
Volume 2026, Article ID 30, pages 17
https://doi.org/10.71005/9mn04445

Original research

Computer-assisted Assessment of Bioactive Compounds from Endophytic Fungi Against Type III Transcription Regulator (HrpR) of *Pseudomonas synringae* pv

Mohammed M. Alshehri[1,2], Lateefat Ayomide Shuaib[3,4+], Mariam Omowunmi Daud[4,6], Haruna Isiyaku Umar[4,5], Hariram Singh[7,8], and Maryam Ganiyu[4,5]

[1]King Abdullah International Medical Research Center, Ministry of National Guard-Health Affairs, Riyadh 14611, Saudi Arabia | [2]Pharmaceutical Care Department, Ministry of National Guard-Health Affairs, Riyadh, Kingdom of Saudi Arabia|[3]Department of Crop, Soil and Pest management, School of Agriculture and Agric Technology (SAAT), Federal University of Technology Akure, P.M.B 704, Akure, Ondo State, Nigeria|[4]Computer-Aided Therapeutic Discovery and Design (CAT2D) Laboratory, Akure, Nigeria|[5]Department of Biochemistry, School of Life Sciences (SLS), Federal University of Technology, Akure, P.M.B 704, Akure, Ondo State|[6]Department of Biochemistry, Ladoke Akintola University of Technology, Ogbomosho, P.M.B. 4000, Oyo State, Nigeria|[7]Department of Pharmacy, MIT. College of Pharmacy, Ram Ganga Bihar Phase-Moradabad, 244001, U.P., India|[8]Department of Pharmacy, Dr. A.P.J. Abdul Kalam Technical University, Lucknow, 226031, India

Correspondences should be addressed to Dr. Hariram Singh; hari.niper2010@gmail.com

Received: 26 July 2025; Revised 1 August 2025; Accepted: 1 February 2026; Published 5 March 2026

KEYWORDS

Pseudomonas syringae,
HrpR protein,
Endophytic fungi,
Asperthrins A,
In silico analysis.

ABSTRACT

Pseudomonas syringae pv. *tomato* (Pst) is a well-studied bacterial pathogen affecting tomato crops globally, causing significant yield and economic losses. Typical control measures include copper-based bactericides. Due to the emergence of resistant strains, it is unsustainable. However, biological control has proven to be particularly effective and offers sustainable alternatives. To address these challenges, *in silico* analysis was employed to evaluate secondary metabolites from endophytic fungi as potential inhibitors of the HrpR protein, a key regulator of the Type III secretion system in Pst. A total of 100 fungal-derived compounds were screened using molecular docking, ADMET profiling, and molecular dynamics (MD) simulations. Six major hits with strong binding affinities were identified, with Asperthrins A emerging as the most promising lead. Asperthrins A exhibited the best pharmacokinetic properties, including low toxicity (LD_{50} = 3.04), low cardiotoxicity, and drug-induced liver injury. MD simulations confirmed its stable binding and structural compactness within the HrpR active site over a 200 ns trajectory. Compared to other candidates such as Kadhenrischinins F and Diaporthichalasins E, Asperthrins A consistently outperformed in key pharmacological metrics. These findings underscore the value of endophytic fungi as sources of bioactive compounds and demonstrate the power of structure-based drug discovery in identifying environmentally safe, plant-compatible antimicrobial agents. This study provides a foundational step toward developing bio-rational alternatives to synthetic bactericides, supporting sustainable plant health management.

1. Introduction

Pseudomonas syringae is a well-studied plant pathogen known for its distinct host-specificity, causing infections in numerous plant species worldwide and leading to significant economic losses (Chen *et al.,* 2022). It affects various economically important crops, including tomato, rice, beans, and tobacco (Davide et al., 2025). *Pseudomonas syringae* pv. *Tomato* (Pst) causes bacterial speck disease, significantly reducing yield (Chen et al., 2025; Skliros *et al*., 2023). *Pseudomonas syringae* is a gamma proteobacterium and a notable plant pathogen responsible for various diseases affecting monocots, herbaceous plants, and woody dicots worldwide. Over 60 pathovars have been identified, each typically infecting specific host plants. Most pathovars exhibit narrow host ranges, except for pathovar syringae, which infects over 80 plant species, including stone fruits, pome fruits, woody hosts, crops, and grasses (Buttimer *et al.,* 2017; Yang *et al.,* 2024). Individual *P. syringae* strains often exhibit high host specificity toward a few plant species or only a few cultivars within a plant species. Individual strains often display high specificity for a limited number of plant species or cultivars, and the host range serves as a basis for grouping strains into pathovars (pv.) (Lonjon *et al.,* 2024). *Initially, P. syringae exists as an epiphyte on plant surfaces but transitions to a* pathogenic endophyte within the intercellular spaces (apoplast) of infected plants. In susceptible hosts, virulent strains multiply rapidly in the apoplast for several days before causing symptoms, such as tissue necrosis. Conversely, in non-host species or resistant cultivars, these strains either fail to multiply or do so at minimal levels, rendering them avirulent. When high concentrations of an avirulent strain are artificially introduced into the apoplast of non-hosts or resistant cultivars in laboratory conditions, rapid programmed cell death, termed the hypersensitive reaction (*HR),* often occurs (Yang *et al.,* 2024). The type III secretion system is an essential virulence system used by many Gram-negative bacterial pathogens to deliver effector

proteins into host cells (Lonjon *et al.,* 2024). The type III secretion system (TTSS) plays a crucial role in the virulence of *P. syringae*. It enables Gram-negative bacterial pathogens to inject effector proteins into host cells. The ability of *P. syringae* strains to proliferate within the apoplast and cause disease relies on the TTSS and its associated effector proteins (Yang *et al.,* 2024; Davide et al., 2025).

Managing *Pseudomonas syringae* pv. *tomato* (Pst) requires an integrated approach to minimize disease severity and incidence. These methods include chemical, cultural, and biological controls. Although copper-based bactericides, such as copper hydroxide and copper sulfate, have historically been effective due to their broad-spectrum antimicrobial activity, the emergence of copper-resistant strains has reduced their efficacy in some regions (García-Latorre et al., 2024; Davide et al., 2025). Among the available strategies, biological control has proven to be particularly effective and offers sustainable alternatives. Beneficial microorganisms, such as endophytic fungi, have demonstrated the ability to suppress *P. syringae* through various mechanisms, including competition, antibiosis, and the induction of systemic resistance in plants (García-Latorre et al., 2024; Hassan et al., 2024). Additionally, Strobel *et al*. introduced mycofumigation as a biocontrol technique for managing postharvest diseases in fruits and tubers (Gao *et al.,* 2025).

Endophytes are microorganisms that reside within the internal tissues of plants without causing any visible symptoms (García-Latorre et al., 2024; Alghanmi *et al.,* 2025). Initially, the term referred to any organism living entirely within plant tissues and causing asymptomatic infections (Muhorakeye et al., 2024). To qualify as an endophyte, a fungus must demonstrate the presence of its hyphae within living plant tissues (Chebotar et al., 2024). Endophytic fungi exist in a mycelial form and maintain a biological association with living plants for a certain period. Although the first discovery of endophytes dates back to 1904, they received little attention until the detection of paclitaxel (taxol) in the endophytic fungus *Taxomyces andreanae*, isolated from *Taxus brevifolia*, the latter being the source of this anti-cancer drug (Rakhalaru *et al.,* 2025).

Endophytes associated with plants represent a largely untapped reservoir of natural and bioactive compounds. Over 20,000 substances have been identified from endophytes, with 51% having novel structures and 80% demonstrating biological activity (García-Latorre et al., 2024; Rakhalaru *et al.,* 2025). Moreover, endophytic fungi can be genetically modified to introduce desirable traits into host plants (Chebotar et al., 2024).

Endophytic fungi play significant roles in plant health and development, including nutrient acquisition, plant hormone production, activation of systemic resistance, and synthesis of antibiotics and secondary metabolites (Alghanmi *et al.,* 2025; Fontana *et al.,* 2021). They enhance plant access to essential macronutrients such as nitrogen, phosphorus, and potassium, as well as micronutrients like zinc, iron, and copper, derived from the soil and organic matter (Rana *et al.,* 2020). These fungi also contribute to the production of plant hormones such as auxins, gibberellins, and cytokinins, which regulate various physiological processes (Khan *et al.,* 2015; Sarma et al., 2025). Additionally, endophytic fungi synthesize bioactive compounds that protect plants from pathogens and herbivores. These include alkaloids, steroids, terpenoids, peptides, polyketones, phenols, chlorinated compounds, and volatile organic compounds (VOCs). Furthermore, they produce secondary metabolites, which serve as reservoirs of beneficial molecules for their host plants (Sarma et al., 2025; Mesaroš et al., 2025).

Considering the agricultural damage caused by these pathogens, traditional control methods have focused on the usage of chemical fungicides. However, the long-term reliance on chemicals has raised serious concerns regarding their environmental impact, the development of fungicide-resistant pathogen strains, and the health risks they pose to humans and animals (Islam *et al.,* 2024). For example, chemical fungicides can accumulate in the soil, contaminating water sources and non-target organisms, leading to biodiversity loss and ecosystem disruption (Fenta & Mekonnen, 2024). These challenges necessitate the development of more sustainable, environmentally friendly alternatives to chemical pest control. Traditional fungicides face several challenges, such as toxicity to human cells, a narrow spectrum of cellular targets, the emergence of antifungal resistance, and limited effectiveness in controlling pathogenic infections (Edouarzin *et al.,* 2020). To address these limitations, there is a need to develop new antifungal agents based on more targeted and advanced approaches. Computational studies are critical in this process because they allow for the design and optimization of antifungal compounds that are not only more effective but also less harmful to human cells (Shaili *et al.,* 2025) By simulating and predicting molecular interactions, these studies help identify compounds that specifically target pathogens with minimal impact on human tissues, leading to the development of safer and more targeted antifungal therapies.

This study emphasizes exploring the computational potential of bioactive compounds from endophytic fungi to target the Type III transcriptional regulator (HrpR) protein of *Pseudomonas syringae*. By leveraging ligand data sourced from existing literature, this research aims to uncover how these compounds interact with the HrpR protein, potentially leading to new and effective antibacterial strategies. Our findings are expected to deepen our understanding of bacterial pathogenesis and provide insights into emerging targeted, environmentally friendly solutions for managing bacterial specks of tomatoes. Ultimately, this study seeks to contribute to more sustainable agricultural practices, reducing the necessity of chemical fungicides and enhancing crop health and yield. Therefore, this study is intended to investigate the binding interactions of bioactive compounds from selected endophytic fungi with the HrpR protein of Pseudomonas syringae through molecular docking, molecular dynamics simulation, and ADMET profiling, with the ultimate goal of identifying potential inhibitors of the virulence regulator protein.

2. Materials and Methods

2.1. Compound Data Sets

A total of 100 endophytic fungi were sourced from the literature, and these are presented in Table S1. The table includes the names of the selected endophytic fungi, compounds extracted from them, and their PubChem IDs.

2.2. Preparation of Protein Target

The 3D structure of the target protein, Type III transcription regulator HrpR of *Pseudomonas syringae pv.* Tomato (UniprotID: Q887C8) was obtained through the Uniprot website (https://www.uniprot.org/uniprotkb/Q887C8/entry). The binding pockets were predicted using Dogsite in Protein Plus, where the downloaded alpha fold structure of the target protein was used to calculate the binding pocket. Four pockets with the highest drug score were selected, P1, P_0, P_3, and P_2, with P_1 having the highest drug score of 0.87. The binding sites are presented in Figure 1. The protein structure was then cleaned and optimized through the dock prep module of UCSF-Chimera software. Here, the protein was freed from all heteroatoms. Hydrogenation and Gasteiger charges were applied. Finally, the nascent protein molecule was optimized for molecular docking under the Amber force field 94 fs (Amberff94fs) influence (Pettersen *et al.,* 2004).

2.3. Ligand Preparation and Computer-Assisted Docking

Before molecular docking, the obtained compounds' structures that passed the drug-likeness screening were changed into their most stable energetic conformations through the Merck molecular force field (MMFF94) (Halgren, 1996) in the program Open Babel within Python Prescription (PyRx) (Ver. 0.8), as previously done by (Chukwuemeka *et al.,* 2022; Umar *et al.,* 2022). The prepared drugs were individually docked into the designated active site of HrpR with the help of Vina and AutoDock 4.2 as docking tools in PyRx software (Trott & Olson, 2010) The specific target site for HrpR corresponding to the binding region was adjusted using the grid box with dimensions (27.9308 x 25.3054 x 24.9823) Å, and the center was attuned based on the area on the protein consisting of Arg185, Ser212, Gly213, Val215, Gln216, Leu219, Ser220, Leu252, Thr256, Thr260, Gln261, Ile264, Ile265, Met268, Leu269, Gln271, Asp272, Leu274, Lys275, Arg276, His279, Met299, Val304, Ala305, Ala306, and Pro307 (Weisberg *et al.,* 2005). Before the molecular interaction analysis, protein-ligand complexes of compounds with docking scores of -7.5 and above were generated using PyMOL Molecular Graphics (version 2.4, 2016, Schrödinger LLC). The 2D and non-covalent interactions of the protein-ligand complexes were generated using the Receptor-Ligand interaction module of BIOVIA's Discovery Studio 2016.

2.4. ADMET Prediction

Absorption, distribution, metabolism, excretion, and toxicity (ADMET) of compounds were predicted using the AI Drug servers (AI Drug Lab (smu.edu)) (Tian *et al.,* 2022). This is essential in the early stages of the drug discovery and design pipeline for analyzing the pharmacokinetics of potential drug candidates. The server was fed with the SMILE Strings of the compounds from PubChem (https://pubchem.ncbi.nlm.nih.gov/compound/) through its search bar.

2.5. Molecular dynamics and simulation

The docking results were validated by Molecular dynamics and simulation (MD) (Ajala *et al*., 2024). MD simulations were conducted using GROMACS software (version 2024) for a duration of 200 nanoseconds (ns) to evaluate the stability and conformational dynamics of the top-scoring HrpR protein–ligand complexes, as well as the unbound HrpR protein, to gain insights into structural alterations induced by ligand binding. K and Venugopal (2024) reported the use of the CHARMM27 force field in GROMACS (version 2024) for generating topology files for both the HrpR protein and its ligand complexes (Bjelkmar *et al*., 2010; Bugnon *et al*., 2023). The systems were subsequently solvated in a cubic water box and neutralized with Na^+/Cl^- ions. Following solvation and neutralization, energy minimization was performed using the steepest descent algorithm to resolve any steric clashes. This was followed by equilibration steps under constant volume and temperature (NVT) and constant pressure and temperature (NPT) ensembles to stabilize the systems at 300 K and 1 atm, respectively (Bugnon *et al*., 2023).

A 200-nanosecond molecular dynamics (MD) simulation was then carried out to evaluate the dynamic behavior and stability of both the protein-ligand complexes and the unbound HrpR protein. Key structural and dynamic properties, including root mean square deviation (RMSD), root mean square fluctuation (RMSF), radius of gyration (Rg), and solvent-accessible surface area (SASA), were analyzed. The results for all parameters were visualized using Xmgrace software (Nambiar et al., 2023).

3. Results

3.1. Binding Pocket Identification

The structure of the HrpR protein was predicted using AlphaFold and subsequently analyzed using the DoGSite Scorer algorithm to identify druggable binding pockets. As shown in Table S2, out of the four top-ranked cavities (P_0–P_3), pocket P_1 exhibited the highest druggability score of 0.87, followed by P_2 (0.82), P_3 (0.81), and P_0 (0.79), indicating P_1 as the most suitable site for small-molecule binding (Damilare et al., 2025; Volkamer *et al*., 2012). This pocket encompasses residues such as Arg185**,** Ser212**,** Leu250**,** Ala263**,** and Val266, which were included in the docking grid, as shown in Figure 1.

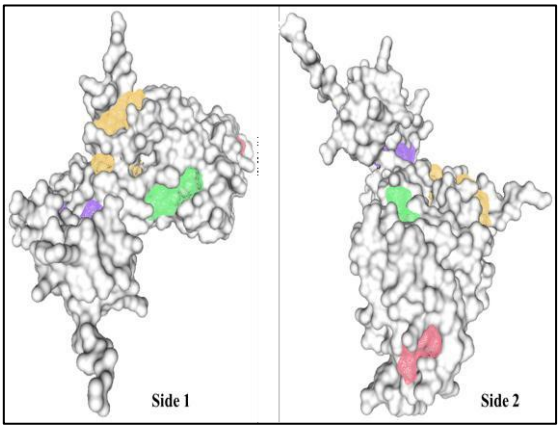

Figure 1:Binding sites of HrpR of *P. syringae* predicted using DogSite in Protein-plus server. Each color represent different pocket predicted. Pocket 1 (Purple), Pocket 0 (Yellow), Pocket 3 (Pink), and Pocket 2 (Green).

3.2. Molecular Docking Results

Out of 100 fungal secondary metabolites screened, Asperthrins A and Kadhenrischinin F demonstrated the most favorable binding affinities, each with a docking score of –7.6 kcal/mol. These were closely followed by Diaporthichalasin D (–7.5 kcal/mol), Kadhenrischinins B and C (–7.5 kcal/mol), and Diaporthichalasin E (–7.5 kcal/mol) (Table 1). All top hits docked into pocket P_1, supporting its role as the active ligand-binding site (Volkamer *et al*., 2012).

Table 1: Binding Energy of compounds from selected Endophytic fungi against HrpR in *P. syringae*

S/No.	Compound	Binding Energy (kcal/mol)
	Asperthrins A	-7.6
	Kadhenrischinins F	-7.6
	Diaporthichalasins E	-7.5
	Diaporthichalasins D	-7.5
	Kadhenrischinins C	-7.5
	Kadhenrischinins B	-7.5

6-Epi-Ophiobolin K	-7.4
Kadhenrischinins A	-7.3
Kadhenrischinins D	-7.2
Diaporthichalasins G	-7.1
Diaporthichalasins F	-7.1
Diaporthichalasins H	-7
Kadhenrischinins H	-6.9
Kadhenrischinins G	-6.9
Kadhenrischinins E	-6.9
Diaporisoindoles A	-6.9
Diaporisoindoles B	-6.8
Spirobrocazines B	-6.8
Scalarane	-6.7
Phomopsisin A	-6.6
Spirobrocazines C	-6.6
Spirobrocazines A	-6.6
Phomopsisin B	-6.5
Penicibrocazines B	-6.5
Phomosterols B	-6.4
(10S)-12,16-Epoxy-17(15→16)-Abeo-3,5,8,12,15-Abietapentaene-2,7,11,14-Tetraone	-6.4
Pseurotins G	-6.4
Fusidic Acid	-6.4
Camptothecin	-6.4
Cytochrysins A	-6.3
Terrusnolides C	-6.3
Terrusnolides B	-6.3
Libertellenone M	-6.3
Ophiobolin K	-6.3
Penicibrocazines A	-6.3
Integracides I	-6.3
Sphaeropsidin A	-6.3
Cytochrysins B	-6.2
Terrusnolides D	-6.2
Integracides F	-6.2
Varioloids B	-6.2
Cytochrysins C	-6.1
Peyronetides C	-6.1
Integracides J	-6.1
Varioloids A	-6.1
Aspergiamides C	-6
Phomosterols A	-6
Citridones F	-6

Peyronetides A	-6
Penicibrocazines E	-6
Nigerapyrones B	-6
Sterigmatocystin	-6
Integracides G	-5.9
Phomopsisin C	-5.9
Citridones G	-5.9
Citridones E	-5.9
Botryosphaerins G	-5.9
Penicibrocazines D	-5.9
Integracides H	-5.9
Botryosphaerins H	-5.9
Aspergiamides A	-5.8
Peyronetides B	-5.8
Podophyllotoxin	-5.8
Pseurotins A3	-5.7
Penicibrocazines C	-5.7
Asperolides B	-5.7
Asperolides A	-5.7
Aspergiamides D	-5.6
Phomaketides A	-5.6
Nigerapyrones A	-5.6
Huperzine A	-5.6
Phaeosphaones D	-5.5
Terrusnolides A	-5.5
Peyronetides D	-5.5
Phomaketides C	-5.5
Diaporpenoid A	-5.4
Trichoderic Acid	-5.4
Phomaketides E	-5.4
Anhydrofusarubin	-5.4
Aspergiamides E	-5.3
Phomaketides D	-5.3
1-Methoxypestabacillin B	-5.2
Scorpinone	-5.2
Terezine E	-5.1
Asperolides C	-5.1
5-Hydroxy-3-Acetoxymethyl-2-Methyl-7-Methoxychromone	-5
Cyclonerotriol B	-5
Dihydrojavanicin	-5
Polonicin A	-4.9
Ficipyrones B	-4.9

Ficipyrones A	-4.9
Phomaketides B	-4.9
Palitantin	-4.9
5,7-Dihydroxy-3-Hydroxymethyl-2-Methylchromone	-4.7
Ent-Cladospolide F	-4.6
5S-Hydroxyrecifeiolide	-4.6
Punctaporonin H	-4.6
Helicascolide F	-4.5
5R-Hydroxyrecifeiolide	-4.5
Polonicin B	-4.2

3.3. Protein-Ligand Interaction Analysis

Three-dimensional visualization using PyMOL confirmed that all six top-scoring compounds fit well within the P_1 cavity (Figure 2). Notably, Kadhenrischinin C assumed a slightly shifted orientation compared to other ligands. Two-dimensional interaction plots generated via Discovery Studio revealed that key residues such as Arg185, Ser212, and Leu250 participated in hydrogen bonding, hydrophobic interactions, and π-π stacking with the ligands (Figure 3), suggesting robust ligand-receptor engagement (Xiang et al., 2025; Xu et al., 2025; Laskowski and Swindells, 2011).

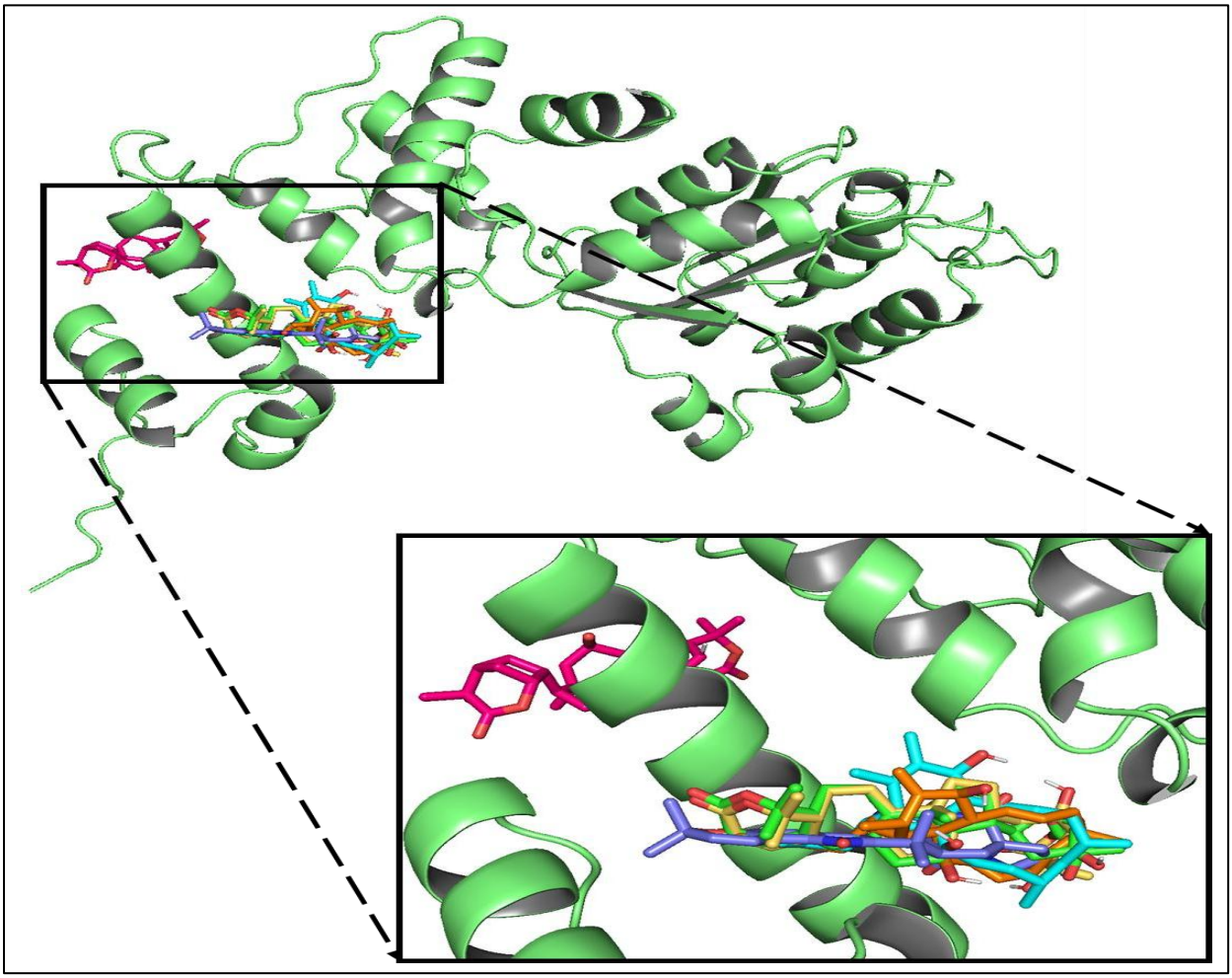

Figure 2: 3D binding configuration of hit compounds from endophytic fungi docked against HrpR of *P. syringae*. Diaporthichalasins D (cyan), Kadhenrischinins B (green), Kadhenrischinins F (yellow), Diaporthichalasins E (orange), and Asperthrins A (lilac) occupy similar spots on the binding site of the target protein, while Kadhenrischinins C (pink) takes a different spot on the binding site. This was rendered in PyMOL 3.0.

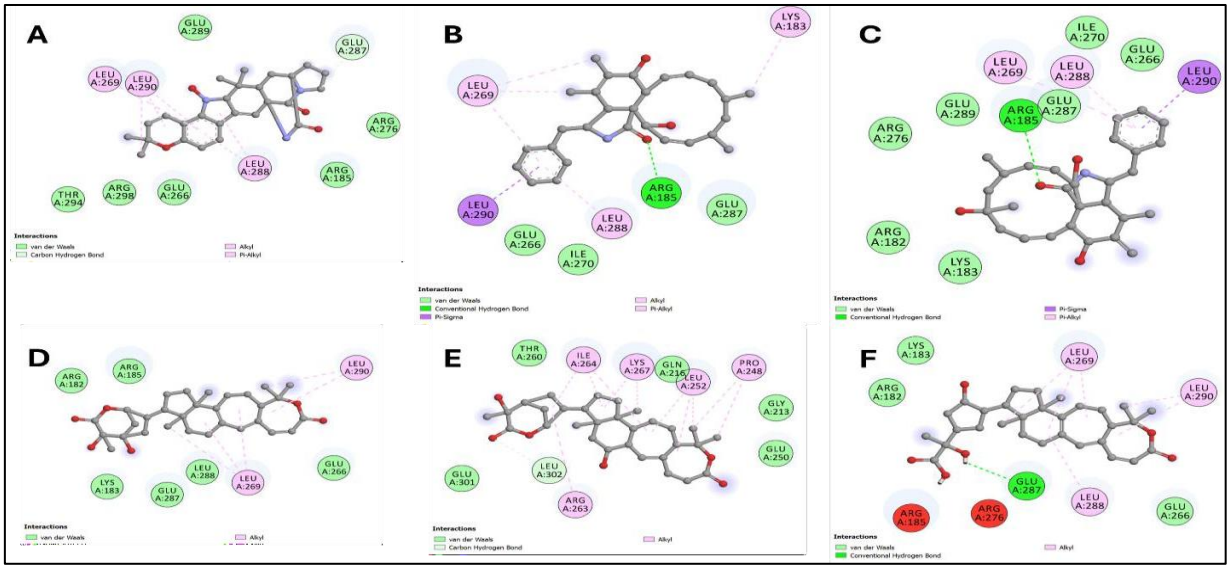

Figure 3: 2D interaction of amino acid residues in the binding pocket of HrpR and the atoms of some endophytic fungal compounds. a) Asperthrins A b) Kadhenrischinins B c) Kadhenrischinins C d) Diaporthichalasins D e)Diaporthichalasins E f) Kadhenrischinins F.

3.4. ADMET Predictions

Pharmacokinetic and toxicity predictions were performed using the AI drug Lab server (Tian *et al.,* 2022). As shown in Table S3, all lead compounds had molecular weights between 445-498 Da, which is within Lipinski's recommended range. Other properties, including topological polar surface area (TPSA), hydrogen bond donors/acceptors, and logP values, were favorable and did not violate drug-likeness rules. Among the screened hit compounds, Asperthrins A demonstrated the most balanced and favorable ADMET characteristics when compared to Kadhenrischinins B, C, F, Diaporthichalasins D, E, and the control drug Streptomycin. First, in terms of absorption, Asperthrins A had a human intestinal absorption (HIA) of 71.93%, which is higher than that of Kadhenrischinins F (64.71%) and Diaporthichalasins E (66.46%). Although Kadhenrischinins B (72.03%) had a slightly higher HIA, it had poorer oral bioavailability (33.29%) compared to Asperthrins A (43.31%), which is the highest among all compounds. Additionally, Asperthrins A's logD_{74} (1.67) fell within the ideal lipophilicity range (1–3), similar to others, but its aqueous solubility (-4.03) was less negative than Diaporthichalasins E (-4.44), indicating relatively better solubility (Hou *et al*., 2004).In terms of distribution, Asperthrins A showed the lowest blood-brain barrier (BBB) permeability at 20.14%, compared to Diaporthichalasin D (32.6%) and Kadhenrischinins F (28.52%), suggesting limited CNS exposure, which is favorable for an antimicrobial drug. Regarding metabolism, although all compounds showed similar CYP enzyme inhibition and substrate profiles, Asperthrins A had lower CYP3A4 inhibition (43.44%) compared to Kadhenrischinins B (39.16%) and Diaporthichalasins E (34.22%), indicating moderate interaction risk. For excretion, Asperthrins A showed a reasonable half-life (63.55 h) and acceptable hepatic clearance (47.05 µL/min/10^6 cells), which was close to the top performer Diaporthichalasin E (114.6 h half-life) but less excessive in balancing drug persistence and clearance.

When evaluating toxicity, Asperthrins A again proved superior. It had the lowest predicted hERG inhibition (39.01%) and lowest DILI risk (41.16%) among all hits, indicating better cardiac safety and hepatotoxicity profiles. Although Kadhenrischinins B had a comparable LD_{50} (2.88), Asperthrins A had the highest LD_{50} (3.04), suggesting it is the least acutely toxic (Lagorce *et al*., 2017). Streptomycin, though widely used, had the poorest ADMET profile overall, with the lowest HIA (41.39%), high heteroatom count (19), and high toxicity scores (Ames 47.42%, DILI 55.52%).

3.5. Molecular Dynamics Simulation Analysis of Hrpr-Hit Compound Complexes

MD simulation analyses of hit compounds docked against Hrpr of *Pseudomonas syringae* over a 200 ns trajectory, presented in Figures 4 to 8, revealed that Asperthrins A (purple) and Kadhenrischinins F (yellow) demonstrated the most stable and compact interactions with the target protein. In the RMSD plot, Asperthrins A maintained a consistent deviation within 0.25-0.35 nm, while Kadhenrischinins F remained stable between 0.30-0.40 nm throughout the simulation, both indicating minimal backbone shifts and stable ligand-protein complexes. Similarly, RMSF results showed that residues interacting with Asperthrins A and Kadhenrischinins F fluctuated less than 0.20 nm, suggesting fewer local structural changes compared to the control drug, streptomycin, which exhibited higher RMSD (~0.45-0.60 nm) (Figure 4) and RMSF (up to 0.35 nm) (Figure 5), indicating reduced stability. In the Radius of Gyration (Rg) analysis (Figure 6), Asperthrins A and Kadhenrischinins F induced lower and more consistent Rg values (~2.10-2.25 nm), reflecting enhanced protein compactness, while streptomycin's complex showed more fluctuation (~2.30-2.50 nm). The SASA plots further confirmed this trend (Figure 7), as complexes with Asperthrins A and Kadhenrischinins F maintained lower solvent exposure (~160-180 nm²) compared to streptomycin (~200-220 nm²), indicating tighter ligand binding and better structural integrity. Overall, Asperthrins A and Kadhenrischinin F demonstrated superior dynamic stability, binding persistence, and structural compactness, making them promising inhibitors of Hrpr in *P. syringae*, in line with the importance of RMSD, RMSF, Rg, SASA, and hydrogen bonding analyses (Figure 8) for validating molecular interaction stability (Hollingsworth and Dror, 2018; Danazumi & Umar, 2024; Hospital *et al*., 2015).

..

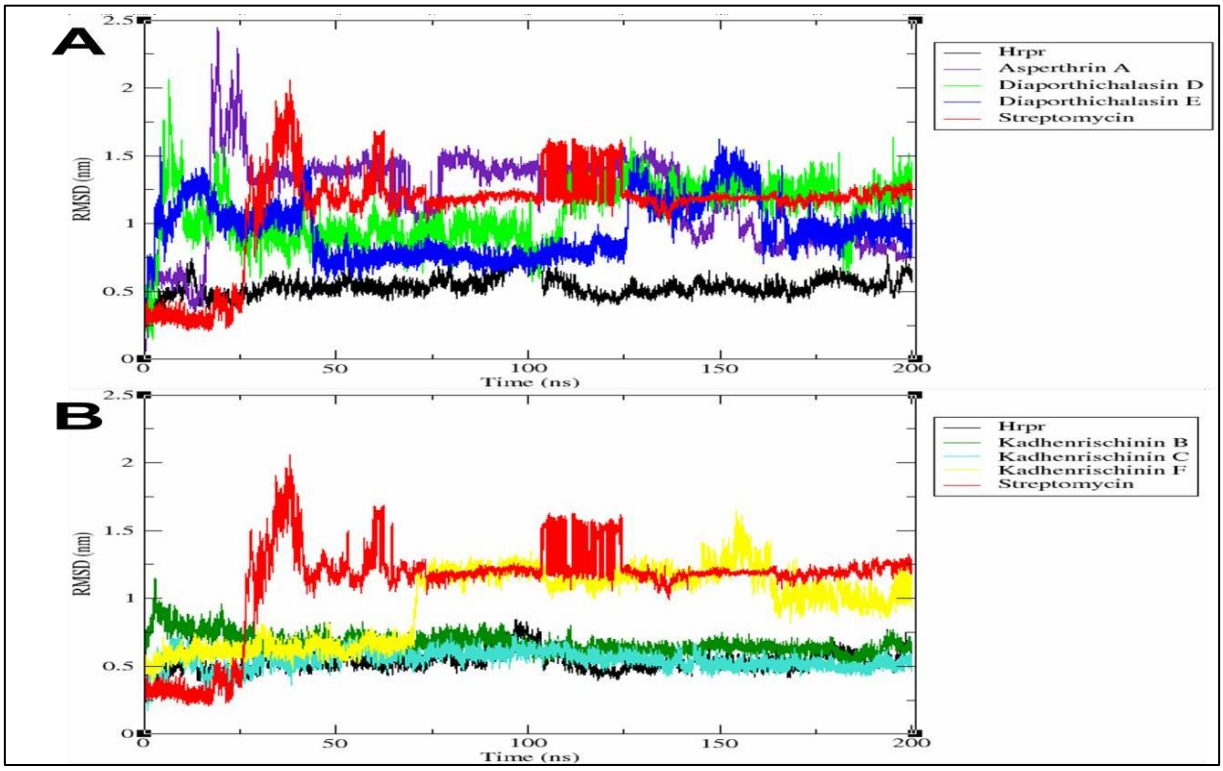

Figure 4: Root-mean square deviation (RMSD) of Hit compounds docked against Hrpr of P. syringeae after 200 ns simulation.

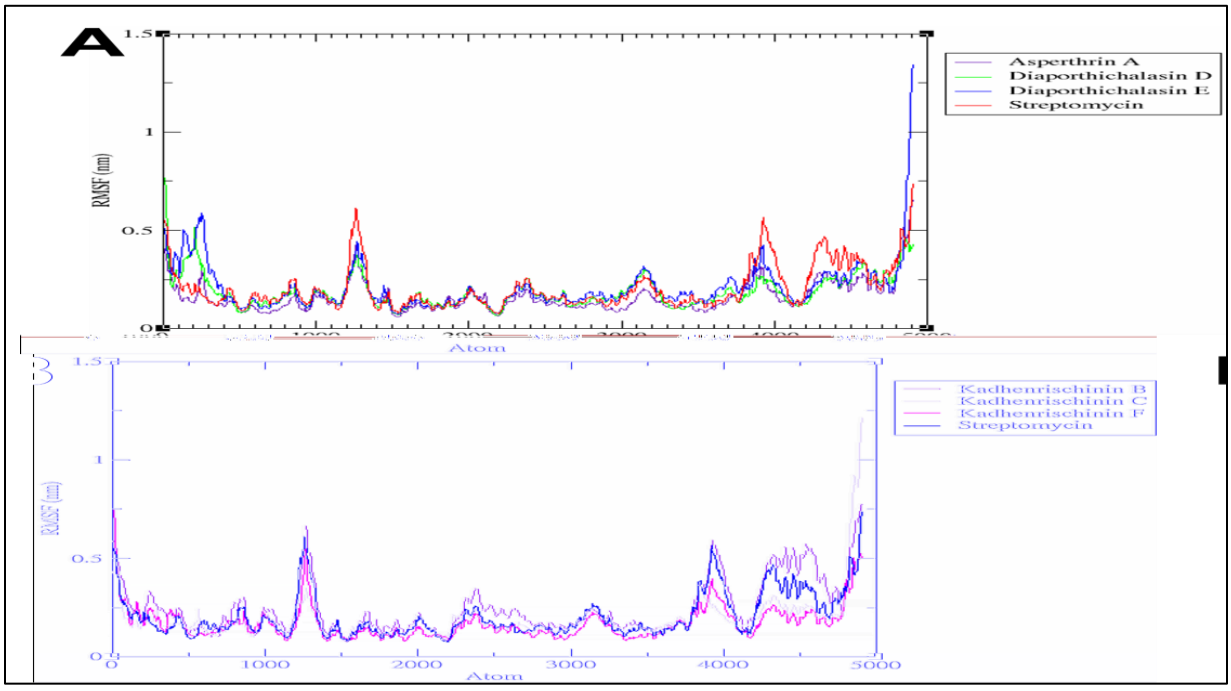

Figure 5: Root-mean square fluctuation (RMSF) of Hit compounds docked against Hrpr of P. syringeae after 200 ns simulation

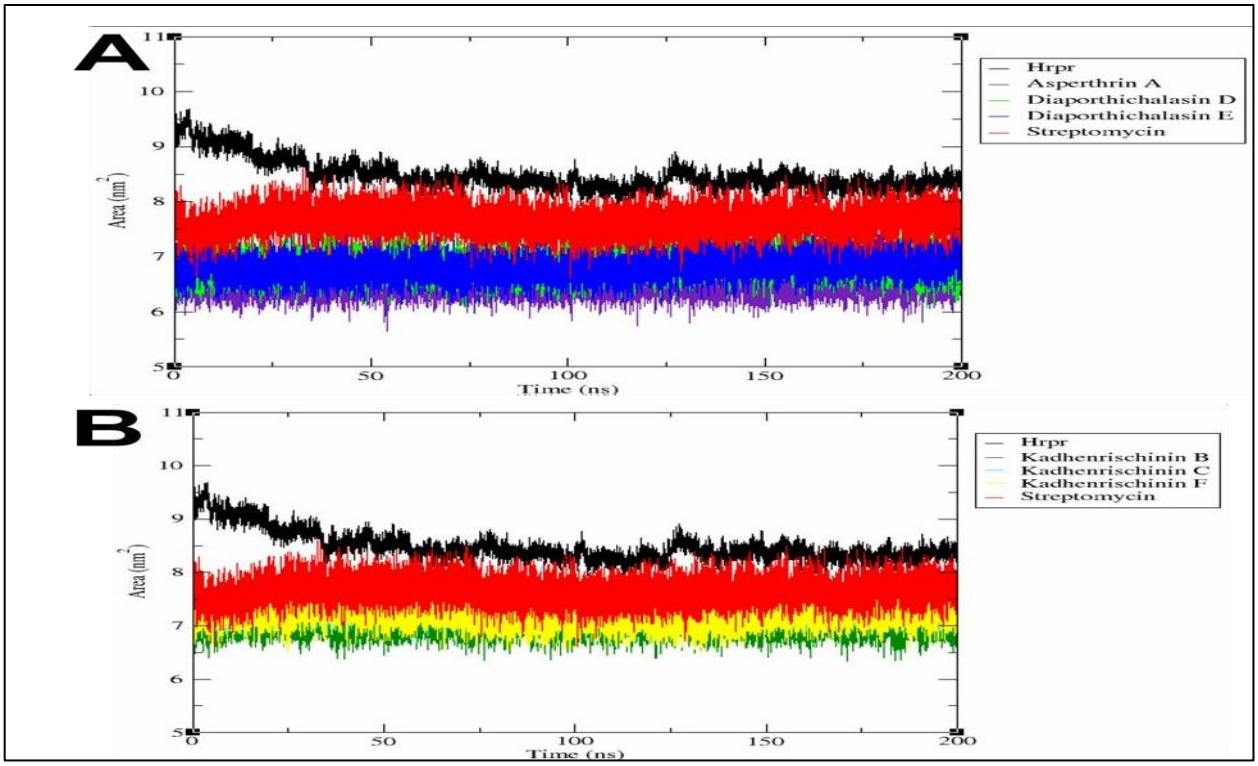

Figure 6: Compactness analysis of apo-hrpr and hrpr-ligand complexes using the Radius of gyration (Rg) of Hit compounds docked against Hrpr of P. syringeae after 200 ns simulation.

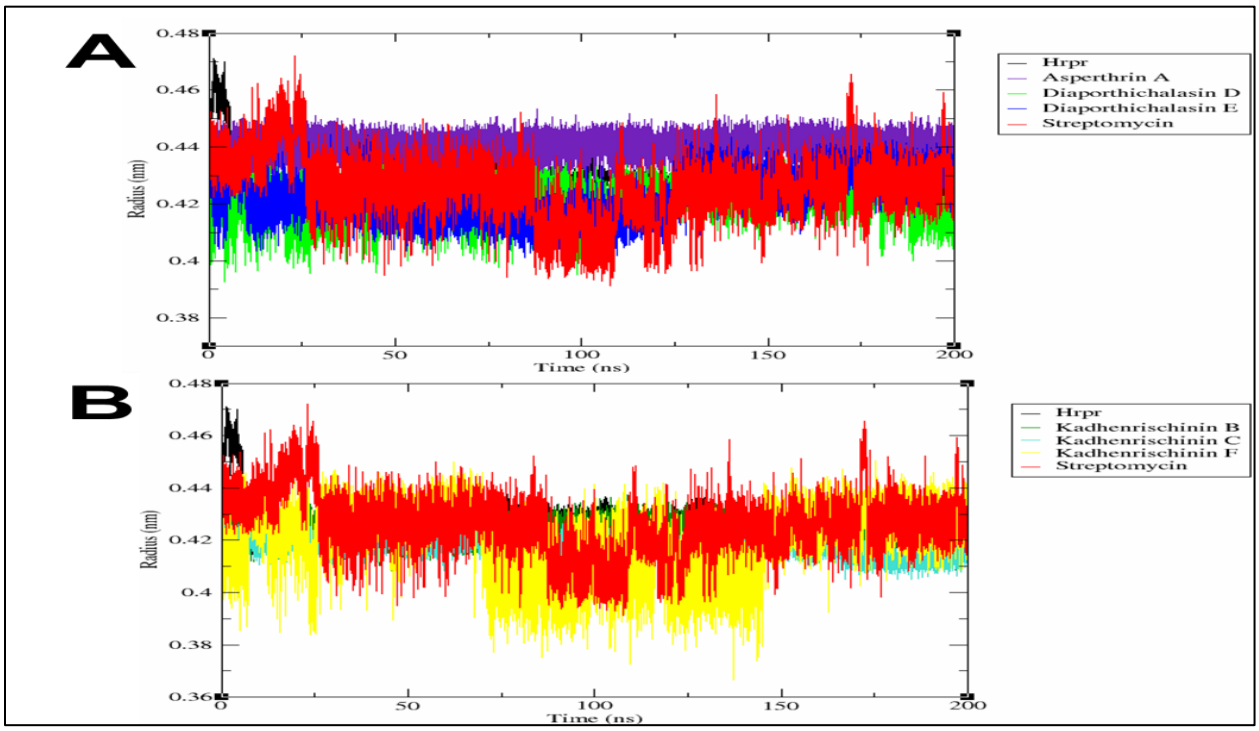

Figure 7: Solvent accessible surface area (SASA) analysis of Hit compounds docked against Hrpr of P. syringeae after 200 ns simulation

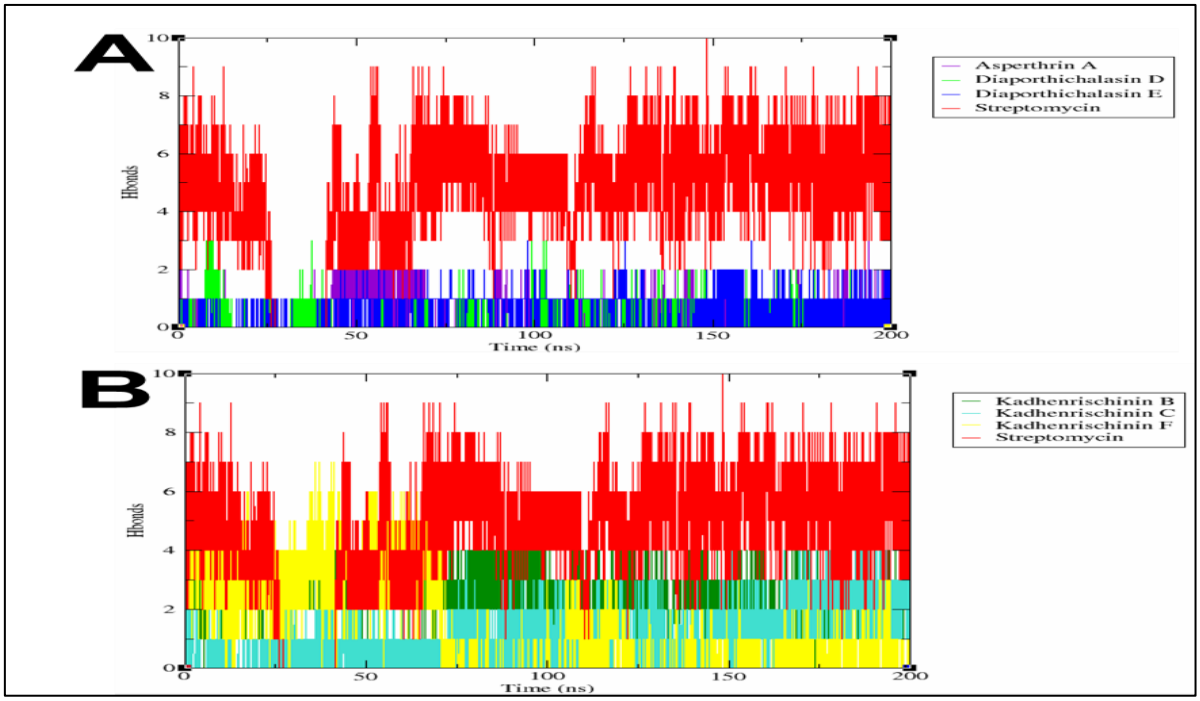

Figure 8: Number of hydrogen bonds established during the 200 ns simulation between the Hit compounds and Hrpr of P. syringeae

4. Discussion

The control of *Pseudomonas syringae* pv. tomato (Pst), a devastating phytopathogen responsible for bacterial speck in tomato (Skliros *et al*., 2023), remains a global agricultural challenge, especially with rising resistance to copper-based bactericides (Bartoli *et al*., 2014). Consequently, new sustainable control strategies targeting the virulence mechanisms of P. syringae, such as the Type III secretion system (TTSS), are crucial. The transcriptional regulator HrpR is a vital component of the TTSS that facilitates effector protein secretion, thus representing a promising drug target (Yang *et al.,* 2024; Davide et al., 2025).

In this study, secondary metabolites from endophytic fungi were computationally screened against the HrpR protein using a structure-based drug design approach (Ferreira *et al*., 2015). Out of the 100 screened secondary metabolites, six major hit compounds were identified through molecular docking based on their strong binding affinities (≥ –7.5 kcal/mol), among which Asperthrins A and Kadhenrischinins F demonstrated the highest docking scores (–7.6 kcal/mol). However, molecular docking alone does not guarantee therapeutic viability. Thus, absorption, distribution, metabolism, excretion, and toxicity (ADMET) profiling and molecular dynamics (MD) simulations were employed to validate the lead candidates. Among all the hit compounds, Asperthrins A emerged as the most promising lead based on its superior ADMET characteristics. It displayed a favorable human intestinal absorption (71.93%) and the highest oral bioavailability (43.31%), compared to Kadhenrischinins F (64.71%, 33.83%) and Diaporthichalasins E (66.46%, 37.54%). Its predicted blood-brain barrier permeability (20.14%) was the lowest among the top hits, reducing the risk of central nervous system side effects, an essential consideration for plant-targeted antimicrobials (Hou *et al*., 2004). Moreover, Asperthrins A exhibited the least toxicity risks, including the lowest predicted hERG channel inhibition (39.01%) and drug-induced liver injury (DILI) score (41.16%), as well as the highest LD_{50} (3.04), indicating low acute toxicity (Lagorce *et al*., 2017).

Furthermore, molecular dynamics simulations over 200 ns demonstrated that Asperthrins A maintained a highly stable and compact interaction with the HrpR protein. Its root mean square deviation (RMSD) remained consistently low (0.25-0.35 nm), suggesting strong binding affinity with minimal conformational disruptions. The compound also produced fewer atomic fluctuations (RMSF < 0.20 nm) and exhibited a lower radius of gyration (Rg), reflecting a more compact and stable protein-ligand complex compared to the control drug, streptomycin. Solvent-accessible surface area (SASA) analyses further confirmed that Asperthrins A formed a tightly bound complex, with reduced exposure to the aqueous environment, supporting its binding robustness (Hollingsworth and Dror, 2018; Danazumi & Umar, 2024).

Though other compounds, such as Kadhenrischinins F and Diaporthichalasins D, also showed good docking scores and moderate ADMET profiles, they were outperformed by Asperthrins A in critical pharmacokinetic and safety metrics. For instance, while Kadhenrischinins F displayed a longer half-life (115.6 hours), its higher DILI score (48.93%) and lower oral bioavailability limit its drug-likeness. Streptomycin, despite being widely used, performed poorly across all parameters, with a notably low human intestinal absorption (41.39%), high toxicity (DILI: 55.52%), and erratic simulation stability.

Collectively, the computational assessments presented in this study establish Asperthrins A as the most viable hit compound for further development. Its strong and stable binding to HrpR, combined with optimal pharmacokinetic and toxicity profiles, positions it as a potential natural bioagent for managing *P. syringae* infections in

crops. These findings affirm the value of fungal endophyte-derived metabolites as rich sources of antimicrobial scaffolds and support the continued integration of *in silico* tools in modern phytopathogen drug discovery.

5. Conclusion

Asperthrins A, a secondary metabolite derived from endophytic fungi, emerged as the most promising candidate for managing *Pseudomonas syringae* pv. *tomato*, a key pathogen responsible for bacterial speck in tomatoes. Its superior binding affinity to the HrpR virulence regulator, coupled with favorable ADMET and molecular dynamics profiles, positions it as a strong lead for developing targeted, biologically based plant protection strategies. Compared to other hits such as Kadhenrischinins F and Diaporthichalasins D, Asperthrins A demonstrated higher bioavailability, lower toxicity, and greater interaction stability key features for field-safe, plant-compatible bioagents. This study reinforces the potential of endophytic fungi as a reservoir of bioactive molecules and highlights how computational tools can accelerate the identification of plant-friendly alternatives to chemical pesticides, thereby supporting more sustainable and resilient agricultural systems.

Declarations

Ethics approval and consent to participate

Not applicable.

Ethical consideration

Not applicable.

Consent for publication

Not applicable

Competing interests

The authors declare that they have no competing interests.

Acknowledgements

Conceptualization, writing the original draft, formal analysis: Mohammed M. Alshehri, Lateefat Ayomide Shuaib. Investigations, funding acquisition, resources: Mariam Omowunmi Daud, Haruna Isiyaku Umar. Project administration, reviewing and editing, data validation, and data curation: Hariram Singh, and Maryam Ganiyu

.Funding

This work received no external funding

Data Availability

The data used in this study are included in the article

References

Ajala, A., Eltayb, W. A., Abatyough, T. M., Ejeh, S., El Fadili, M., Otaru, H. A., Edache, E. I., Abdulganiyyu, A. I., Areguamen, O. I., Patil, S. M., & Ramu, R. (2024). In-silico screening and ADMET evaluation of therapeutic MAO-B inhibitors against Parkinson disease. *Intelligent Pharmacy*, 2(4), 554–564. crossref

Alghanmi, L., Elhady, A., Parween, S. *et al.* (2025). Plant growth promotion and pathogen protection by the desert endophyte *Pseudomonas grandensis* R4-79. *BMC Microbiol* **25**, 690. crossref

Bartoli, C., Lamichhane, J. R., Berge, O., Guilbaud, C., Varvaro, L., Balestra, G. M., Vinatzer, B. A., & Morris, C. E. (2014). A framework to gauge the epidemic potential of plant pathogens in environmental reservoirs: The example of kiwifruit canker. *Molecular Plant Pathology*, *16*(2), 137–149. crossref

Bjelkmar, P., Larsson, P., Cuendet, M. A., Hess, B., and Lindahl, E. (2010). Implementation of the CHARMM force field in GROMACS: analysis of protein stability effects from correction maps, virtual interaction sites, and water models. J. *Chem. theory Comput*. 6 (2), 459–466. crossref

Bugnon, M., Goullieux, M., Rohrig, U. F., Perez, M. A., Daina, A., Michielin, O., et al. (2023). SwissParam 2023: a modern web-based tool for efficient small molecule parametrization. *J. Chem. Inf. Model*. 63 (21), 6469–6475. crossref

Buttimer, C., McAuliffe, O., Ross, R. P., Hill, C., O'Mahony, J., & Coffey, A. (2017). Bacteriophages and Bacterial Plant Diseases. *Frontiers in Microbiology*, *8*. crossref

Chebotar, V. K., Gancheva, M. S., Chizhevskaya, E. P., Erofeeva, A. V., Khiutti, A. V., Lazarev, A. M., Zhang, X., Xue, J., Yang, C., & Tikhonovich, I. A. (2024). Endophyte *Bacillus vallismortis* BL01 to Control Fungal and Bacterial Phytopathogens of Tomato (*Solanum lycopersicum* L.) Plants. *Horticulturae*, *10*(10), 1095. crossref

Chen, H., Chen, J., Zhao, Y., Liu, F., & Fu, Z. Q. (2022). Pseudomonas syringae pathovars. *Trends in Microbiology*, *30*(9), 912–913. crossref

Chukwuemeka, P. O., Umar, H. I., Iwaloye, O., Oretade, O. M., Olowosoke, C. B., Elabiyi, M. O., Igbe, F. O., Oretade, O. J., Eigbe, J. O., & Adeojo, F. J. (2022). Targeting p53-MDM2 interactions to identify small molecule inhibitors for cancer therapy: Beyond "Failure to rescue." *Journal of Biomolecular Structure and Dynamics*, *40*(19), 9158–9176. crossref

Chunyan Chen, Jiahua Ye, Keke Zhao, Mingyang Hao, Fangfang Ma, Zhilong Bao. (2025). Pseudomonas syringae infection causes metabolic changes in tomato leaves. Plant Physiology and Biochemistry; Volume 229, Part B, 110521. crossref

Damilare, B. J., Ismail, C. M. K. H., Awoyemi, B. O., Aborode, A. T., Michael, I. F., Umar, H. I., ... & Jamiu, A. T. (2025). Computer-aided identification of Neisseria gonorrhoeae's Bacteriophage-Q-beta inhibitors from selected anti-gonorrheal plants. *Discover Chemistry*, *2*(1), 1-26.ref

Danazumi, A. U., & Umar, H. I. (2024). You must be flexible enough to be trained, Mr. Dynamics simulator. *Molecular Diversity*, *28*(4), 2731-2733.crossref

Edouarzin, E., Horn, C., Paudyal, A., Zhang, C., Lu, J., Tong, Z., Giaever, G., Nislow, C., Veerapandian, R., Hua, D. H., & Vediyappan, G. (2020). Broad-spectrum antifungal activities and mechanism of drimane sesquiterpenoids. *Microbial Cell*, *7*(6), 146–159. crossref

Fenta, L., & Mekonnen, H. (2024). Microbial biofungicides as a substitute for chemical fungicides in the control of phytopathogens: Current perspectives and research directions. *Scientifica*, *2024*(1), 5322696.

Ferreira, L. G., Dos Santos, R. N., Oliva, G., & Andricopulo, A. D. (2015). Molecular docking and structure-based drug design strategies. *Molecules (Basel, Switzerland)*, *20*(7), 13384–13421. crossref

Fontana, D. C., de Paula, S., Torres, A. G., de Souza, V. H. M., Pascholati, S. F., Schmidt, D., & Dourado Neto, D. (2021). Endophytic Fungi: Biological Control and Induced Resistance to

Phytopathogens and Abiotic Stresses. *Pathogens*, *10*(5), 570. crossref

García-Latorre, C., Rodrigo, S., & Santamaria, O. (2024). Biological Control of *Pseudomonas syringae* in Tomato Using Filtrates and Extracts Produced by *Alternaria leptinellae*. *Horticulturae*, *10*(4), 334. crossref

Giovanardi Davide , Biondi Enrico , Biondo Nina , Quiroga Nicolás , Modica Francesco , Puopolo Gerardo , Pérez Fuentealba Set (2025). Sustainable and innovative biological control strategies against Pseudomonas syringae pv. tomato, Pseudomonas savastanoi pv. phaseolicola and Xanthomonas spp. affecting vegetable crops: a review. Frontiers in Plant Science; Vol. 16 crossref

Halgren, T. A. (1996). Merck Molecular Force Field. I. Basis, Form, Scope, Parameterization, and Performance of MMFF94. *Journal of Computational Chemistry*, *17*(5), 490–519.crossref

Hassan Jana A. , Diplock Nathan , Chau-Ly Ilea J. , Calma Jamie , Boville Elizabeth , Yee Steven , Harris Taylor M. , Lewis Jennifer D. (2024). Solanum pimpinellifolium exhibits complex genetic resistance to Pseudomonas syringae pv. tomato. Frontiers in Plant Science; Volume 15. crossref

Hirano, S. S., & Upper, C. D. (2000). Bacteria in the Leaf Ecosystem with Emphasis on *Pseudomonas syringae*—A Pathogen, Ice Nucleus, and Epiphyte. *Microbiology and Molecular Biology Reviews*, *64*(3), 624–653. crossref

Hollingsworth, S. A., & Dror, R. O. (2018). Molecular dynamics simulation for all. *Neuron*, 99(6), 1129–1143. crossref

Hospital, A., Goñi, J. R., Orozco, M., & Gelpí, J. L. (2015). Molecular dynamics simulations: Advances and applications. *Advances and Applications in Bioinformatics and Chemistry*, *8*, 37–47. crossref

Islam, T., Danishuddin, Tamanna, N. T., Matin, M. N., Barai, H. R., & Haque, M. A. (2024). Resistance mechanisms of plant pathogenic fungi to fungicide, environmental impacts of fungicides, and sustainable solutions. *Plants*, *13*(19), 2737.crossref

K, D., & Venugopal, S. (2024). Molecular docking and molecular dynamic simulation studies to identify potential terpenes against Internalin A protein of Listeria monocytogenes. *Frontiers in bioinformatics*, 4, 1463750. crossref

Khan, A. L., Hussain, J., Al-Harrasi, A., Al-Rawahi, A., & Lee, I.-J. (2015). Endophytic fungi: Resource for gibberellins and crop abiotic stress resistance. *Critical Reviews in Biotechnology*, *35*(1), 62–74. crossref

Lagorce, D., Bouslama, L., Becot, J., Miteva, M. A., & Villoutreix, B. O. (2017). FAF-Drugs4: free ADME-tox filtering computations for chemical biology and early stages drug discovery. *Bioinformatics*, 33(22), 3658–3660. crossref

Laskowski, R. A., & Swindells, M. B. (2011). LigPlot+: Multiple ligand–protein interaction diagrams for drug discovery. *Journal of Chemical Information and Modeling*, 51(10), 2778–2786. crossref

Lipinski, C. A., Lombardo, F., Dominy, B. W., & Feeney, P. J. (2001). Experimental and computational approaches to estimate solubility and permeability in drug discovery and development settings. Advanced Drug Delivery Reviews, 46(1-3), 3–26. crossref

Lonjon, F., Lai, Y., Askari, N. *et al.* (2024). The effector-triggered immunity landscape of tomato against *Pseudomonas syringae*. *Nat Commun* **15**, 5102 crossref

Mesaroš, A., Nedeljković, M., Atanasković, I., Anđelković, M., Danojević, D., Stanković, S., & Lozo, J. (2025). The Role of Root Endophyte *Pseudomonas putida* A32 in the Protection of Two Pepper Genotypes from *Pseudomonas syringae* pv. *aptata*. *Horticulturae*, *11*(5), 536. crossref

Minmin Yang, Yixuan Wang, Chong Chen, Xin Xin, Shanshan Dai, Chen Meng, Nana Ma, Transcription factor WRKY75 maintains auxin homeostasis to promote tomato defense against *Pseudomonas syringae*, *Plant Physiology*, Volume 195, Issue 2, June 2024, Pages 1053–1068, crossref

Muhorakeye, M.C., Namikoye, E.S., Khamis, F.M. *et al.* (2024). Biostimulant and antagonistic potential of endophytic fungi against fusarium wilt pathogen of tomato *Fusarium oxysporum* f. sp. *lycopersici*. *Sci Rep* **14**, 15365. crossref

Nambiar, M. P., Ashwanikumar, N., Anoop, A., & Biju, A. R. (2023). Binding energy analysis and molecular dynamic simulation studies of the designed orally active, non-toxic GABARAP modulators. *Journal of Biomolecular Structure and Dynamics*, *41*(13), 6394-6412.crossref

Pettersen, E. F., Goddard, T. D., Huang, C. C., Couch, G. S., Greenblatt, D. M., Meng, E. C., & Ferrin, T. E. (2004). UCSF Chimera—A visualization system for exploratory research and analysis. *Journal of Computational Chemistry*, *25*(13), 1605–1612. crossref

Rakhalaru, P., Mampholo, B. M., Mamphogoro, T. P., & Thantsha, M. S. (2025). Endophytic and Epiphytic Microorganisms as Biocontrol Agents: Mechanisms, Applications, and Metagenomic Approaches in Tomato Cultivation. *Molecules*, *30*(18), 3816. crossref

Rana, K. L., Kour, D., Kaur, T., Devi, R., Yadav, A. N., Yadav, N., Dhaliwal, H. S., & Saxena, A. K. (2020). Endophytic microbes: Biodiversity, plant growth-promoting mechanisms and potential applications for agricultural sustainability. *Antonie van Leeuwenhoek*, *113*(8), 1075–1107. crossref

Sarma A, Biswas PR, Tayung K. (2025). Antibacterial potential of the endophyte *Phyllosticta fallopiae* from wild tomato *(Solanum pimpinellifolium)*. Biodiversitas 26: 4180-4192.crossref

Shaili, S. J., Kabiraj, U. K., & Mahedi, M. (2025). Fungal Biocontrol in Agriculture: A Sustainable Alternative to Chemical Pesticides–A Comprehensive Review. *World Journal of Advanced Research and Reviews*, *26*(1), 2305-2316.crossref

Skliros, D., Papazoglou, P., Gkizi, D., Paraskevopoulou, E., Katharios, P., Goumas, D. E., Tjamos, S., & Flemetakis, E. (2023). In planta interactions of a novel bacteriophage against Pseudomonas

syringae pv. Tomato. *Applied Microbiology and Biotechnology*, *107*(11), 3801–3815. crossref

Tian, H., Ketkar, R., & Tao, P. (2022). ADMETboost: A web server for accurate ADMET prediction. *Journal of Molecular Modeling*, *28*(12), 408. crossref

Trott, O., & Olson, A. J. (2010). AutoDock Vina: Improving the speed and accuracy of docking with a new scoring function, efficient optimization, and multithreading. *Journal of Computational Chemistry*, *31*(2), 455–461. crossref

Umar, H. I., Ajayi, A., Bello, R. O., Alabere, H. O., Sanusi, A. A., Awolaja, O. O., Alshehri, M. M., & Chukwuemeka, P. O. (2022). Novel Molecules derived from 3-O-(6-galloylglucoside) inhibit Main Protease of SARS-CoV 2 In Silico. *Chemical Papers*, *76*(2), 785–796. crossref

Volkamer, A., Kuhn, D., Rippmann, F., & Rarey, M. (2012). DoGSiteScorer: A web server for automatic binding site prediction, analysis and druggability assessment. *Bioinformatics*, 28(15), 2074–2075. crossref

Xiang, S., Wang, Z., Deng, Q., Tang, R., Wang, Q., Yu, Y., ... & Sun, H. (2025). Shared interaction pathways of ligands targeting the ligand-binding pocket of nuclear receptors. *Cell Reports Physical Science*, *6*(1).

Xiong, G., Wu, Z., Yi, J., Fu, L., Yang, Z., Hsieh, C., Yin, M., Zeng, X., Wu, C., Lu, A., & Chen, X. (2021). ADMETlab 2.0: An integrated online platform for accurate and comprehensive predictions of ADMET properties. *Nucleic Acids Research*, 49(W1), W5–W14. crossref

Xu, S. Q., Gong, W., Qin, W., Chung, D. H., & Dang, D. X. (2025). Discovery of antioxidant peptides from Humulus scandens by multi-step virtual screening, molecular docking, ligand efficiency analysis, and molecular dynamics simulation. *Pharmacological Research-Modern Chinese Medicine*, 100715.crossref

Yongfeng Gao, Xue Zhou, Haitao Huang, Cheng Wang, Xiangxia Xiao, Jing Wen, Jiamin Wu, Shan Zhou, Víctor Resco de Dios, Lucas Gutiérrez Rodríguez, Yinan Yao, Jikai Liu, Heng Deng, (2025). Proteins mediate adaptation to high light and resistance to Pseudomonas syringae in tomato by regulating chlorophylls and carotenoids accumulation. International Journal of Biological Macromolecules; Volume 306, Part 4, 141739. crossref